Eur. Phys. J. B **61**, 413–418 (2008)
DOI: 10.1140/epjb/e2008-00091-3

THE EUROPEAN PHYSICAL JOURNAL B

Atomistic level studies on the tensile behavior of GaN nanotubes under uniaxial tension

Z.G. Wang[1,a], X.T. Zu[1], F. Gao[2], and W.J. Weber[2]

[1] Department of Applied Physics, University of Electronic Science and Technology of China, Chengdu, 610054, P.R. China
[2] Pacific Northwest National Laboratory, P.O. Box 999, Richland, WA 99352, USA

Received 14 August 2007 / Received in final form 1st November 2007
Published online 5 March 2008 – © EDP Sciences, Società Italiana di Fisica, Springer-Verlag 2008

Abstract. Molecular dynamics method with the Stillinger-Weber (SW) potential has been employed to study the responses of GaN nanotubes (GaNNTs) to a uniaxial tensile load along the axial direction. It has been revealed that GaNNTs exhibits a completely different tensile behavior at different temperatures, i.e. ductility at higher deformation temperatures and brittleness at lower temperatures, leading to a brittle to ductile transition (BDT). Both the BDT temperature and the critical stress increases with increasing thickness of GaNNTs, and the critical stress at higher temperature are lower than those at lower temperature. These results on the tensile behaviors of GaNNTs in an atomic level will provide a good reference to its promising applications.

PACS. 62.25.+g Mechanical properties of nanoscale systems – 65.80.+n Thermal properties of small particles, nanocrystals, and nanotubes – 02.70.Ns Molecular dynamics and particle methods

1 Introduction

One dimensional nanostructures, such as nanowires and nanotubes, exhibit novel electronic and optical properties that are intrinsically associated with their low dimensionality and quantum confinement effect [1,2]. One dimensional semiconductor nanostructures are considered to be one of the critical building blocks for nanoscale optoelectronics [3]. To implement these nanoscale building blocks for nanoelectronics, their mechanical behavior must be carefully considered because the potential applications depend on the stability and stiffness of these nanostructures. Wurtzite structure gallium nitride (GaN), a direct band-gap semiconductor (3.4 eV) at room temperature, is an ideal material for fabrication of blue/green light emitting diodes, laser diodes, and high power integrated circuits [4,5]. Recently, successful formations of single crystalline GaN nanotubes (GaNNTs) have been reported. Goldberger and co-workers [6] reported an 'epitaxial casting' approach for the synthesis of single-crystal GaNNTs with the inner diameters of 30–200 nm, the wall thicknesses of 5–50 nm. The cross-section of the GaNNTs is hexagonal, with their axial direction of the GaNNTs along [001] direction, but the normal of lateral facets is along [110] direction. Liu et al. [7] have prepared single-crystalline GaNNTs using a chemical thermal evaporation process, but the side surfaces of GaNNTs mainly consist of (100) planes, which is also more stable than that with side surfaces of (110) planes. Hu et al. [8] reported the growth of GaNNTs in bulk by a two-stage process based on a well-controllable conversion of amorphous gallium oxide (Ga_2O) nanotubes. And Hung et al. [9] reported the formation of GaNNTs with inner diameter of 40 nm and wall thicknesses of 40 nm by inductively coupled plasma etching on a GaN template. The GaNNTs were hexagonal with the [001] direction perpendicular to the substrate surface. The binary materials composed of Group III nitrides are viewed as ideal analogs of carbon because of their isoelectrons in a hexagonal network and potential used in light emitting device. The mechanical properties of carbon nanotubes have been investigated extensively [10–13]. However, relatively few studies have attempted to a detailed investigation on the GaNNTs mechanical properties. Although Jeng et al. [14] have reported the mechanical properties of GaNNTs, they were based on hypothetical single-walled GaNNTs, and do not accurately model realistic single-crystalline GaNNTs. Our previous simulation results show that GaNNTs with side surfaces of (110) planes exhibit completely different tensile behavior at different temperatures, i.e. ductility at higher temperatures and brittleness at lower temperatures, leading to a brittle to ductile transition (BDT) [15]. The recent experiment shows that GaNNTs consist of (100) planes is more stable than that with side surfaces of (110) planes. In the present study, we employs classical molecular dynamics methods based on the Stillinger-Weber potential to perform a comprehensive investigation into the tensile behavior of single-crystalline GaNNTs with side surfaces of (100) planes.

[a] e-mail: zgwang@uestc.edu.cn

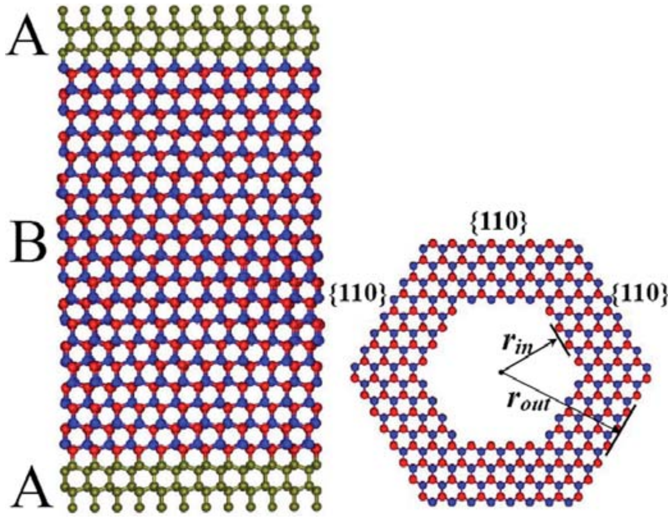

Fig. 1. (Color online) Top view of [001]-oriented GaNNTs with [100] oriented lateral facets. The axial direction of the nanotubes is along [001] direction. And initial configuration of GaNNTs for tensile test. Label "*A*" denotes the free motion region and "*B*" indicates the tension region.

2 Simulation details

A classical MD method was employed in this work and the *NVT* ensemble (constant volume and temperature) was employed. Atomic interactions of GaN are described by a Stillinger-Weber (SW) form [16], where the potential parameters used in the present study were developed by Kioseoglou et al. [17]. The potentials reproduce the correct binding energy, lattice constants, and elastic properties of wurtzite GaN, and achieve a realistic description of the microscopic structure and the energetic of different planar defects and their interactions in the wurtzite GaN. Furthermore, these potentials have been applied successfully to evaluate the Young's modulus of defect-free and defected single-crystal GaNNTs [18,19], and the melting behavior of GaNNTs [20]. Therefore, these potentials are considered suitable to study the tensile behavior of GaNNTs. In this work, the GaNNTs are generated by cutting the outside and inside parts of a large hexagonal GaN, as described previously [20]. To investigate the atomic structures of single crystalline GaNNTs as observed in experiments [7], GaNNTs with [100]-oriented lateral facets, and with an inner radius of 11.97 Å, are used in the present study. The wall thicknesses of these nanotubes are 3.68, 6.45 and 9.21 Å, and the corresponding numbers of atoms are 2880, 4752, and 6912, respectively. Length (L) of 61.2 Å is used for all the GaNNTs considered. The top view of GaNNTs with [100]-oriented lateral facets is shown in Figure 1b. Strain-stress simulations have been performed using the following procedure: the three atomic layers at the top and bottom of GaNNTs are fixed during simulations, forming two rigid borders that are marked as 'A' regions in Figure 1a. The initial structures of the GaNNTs were equilibrated for 100 ps at a given temperature, which allows the GaNNTs to have stable configurations. The strain was then applied along the tube direction to study the mechanical properties of the GaNNTs, with a displacement of Δz. The atoms in the rigid borders were displaced by $\Delta z/2$, and the coordinates of remaining atoms were scaled by a factor $(L + \Delta z)/L$ along the z direction. This deformed tube was relaxed for 20 000 steps (10 ps), and then the relaxed tube was used as an initial configuration for the next MD simulation. The procedure was repeated until the tube failed (ruptured).

The following scaling method is adopted to ensure that the temperature of the system remains constant during simulation [21]:

$$v_i^{new} = v_i \sqrt{\frac{T_D}{T_R}}, \tag{1}$$

where v_i^{new} is the velocity of particle i after correction. T_D and T_R are the desired and actual temperatures of the system, respectively. This scaling method is applied during the simulation for specific equilibrium temperature.

The localized axial stress state for atom i is defined as

$$\eta_z^i(\varepsilon_z) = \frac{1}{V_i}\left(m_i v_z^i v_z^i + \frac{1}{2} \sum_{\substack{j=1 \\ (j \neq i)}}^{N} F_z^{ij}(\varepsilon_z) r_z^{ij}(\varepsilon_z) \right) \tag{2}$$

where m_i is the mass of atom i. v_z^i is the velocity along the [001] direction. F_z^{ij} refers to the [001] component of the interatomic force between atoms i and j. r_z^{ij} is the interatomic distance in the [001] direction between atoms i and j. V_i refers to the volume of atom i, which was assumed as a hard sphere in a closely packed undeformed crystal structure. The axial stress on the GaNNTs is taken as the arithmetic mean of the local stresses on all atoms, as follows:

$$\sigma_z = \frac{1}{N} \sum_{i=1}^{N} \eta_z^i. \tag{3}$$

The normal strain in the axial direction ε is calculated as

$$\varepsilon_z = \frac{\overline{l_{z(t)}} - l_{z(0)}}{l_{z(0)}} \tag{4}$$

where $\overline{l_{z(t)}}$ is the average length in the axial direction and $l_{z(0)}$ is the average initial length. The strain rate is calculated as

$$\dot{\varepsilon} = \frac{\varepsilon_z}{s\Delta t} \tag{5}$$

where s is the number of relaxation steps after each strain increment and Δt is the simulation time step. In this simulation, the simulation time step was fixed at 0.5 fs. The number of relaxation steps was fixed at 20 000 steps, while the strain increment was varied, using $\varepsilon_z = 0.0005$, i.e. simulating strain rate of 0.005% ps^{-1} was used in this work. The stress during each strain increment was computed by averaging over the final 2000 relaxation steps. The stress-strain relationship of the GaNNTs can be obtained by using equations (3) and (4).

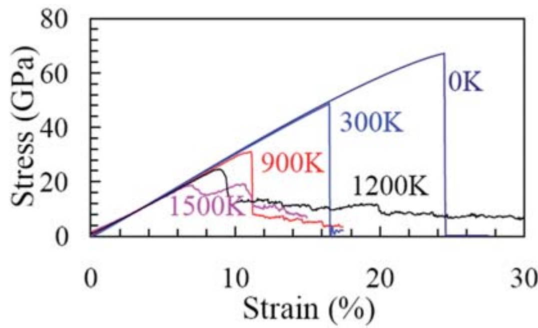

Fig. 2. (Color online) Tensile stress-strain curves of GaNNTs with thickness of 3.68 Å with a strain rate of 0.005%/ps at various temperatures.

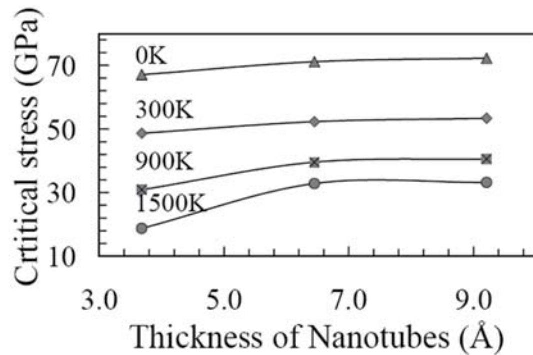

Fig. 3. Dependence of critical stress on the thickness of the GaNNTs. The critical stress increases with the increasing of the thickness of GaNNTs.

3 Results and discussion

Figure 2 shows some representative stress-strain relationship of the GaNNTs with thickness of 3.68 Å, simulated at various temperatures with strain rates of 0.005% ps^{-1}. It is evident that the stress-strain relationship follows the Hooke's law firstly. Then as the strain increases, the stress-strain curves behave non-linearly with a decreasing gradient until a critical strain. Upon reaching the critical strain, the stress experiences an abrupt decrease to about 0 GPa at low temperature and the stress decreases gradually with increasing strain at high temperature; the GaNNTs thus exhibit a brittle behavior at lower temperature and a ductile behavior at high temperature. It was observed that the GaNNTs have lower critical stress and corresponding smaller strain at high temperature than at low temperature. For example the critical stress decreases from 48.66 to 19.11 GPa at temperature increases from 300 to 1500 K. At higher temperature, the atomic structure has high entropy, and its constituent atoms vibrate about their equilibrium position at much larger amplitude, as compared to the low temperature, and hence plastic deformation occurs easily at high temperature.

Figure 3 shows the dependence of critical stress on the thickness of the GaNNTs. As can be seen from the figure that the critical strain increases with the increasing of the thickness of GaNNTs, i.e. the critical stress of the thin one is lower than that of the thick one, which can be regard as resulting from the smallness of the GaNNTs. The critical stress increases from 48.66 to 53.38 GPa and 18.74 to 33.21 GPa with the increase of thickness from 3.68 to 9.21 Å at 300 K and 1500 K, respectively. Generally speaking, the ratio of numbers of surface atoms to the total number of atoms increases as the radius of the GaNNTs reduces. The surface atoms have much more energies than the core ones. So GaNNTs with bigger thickness need more tensile stress to overcome the interaction between atoms. Therefore, the critical stress of large thickness is higher than that of the thin one.

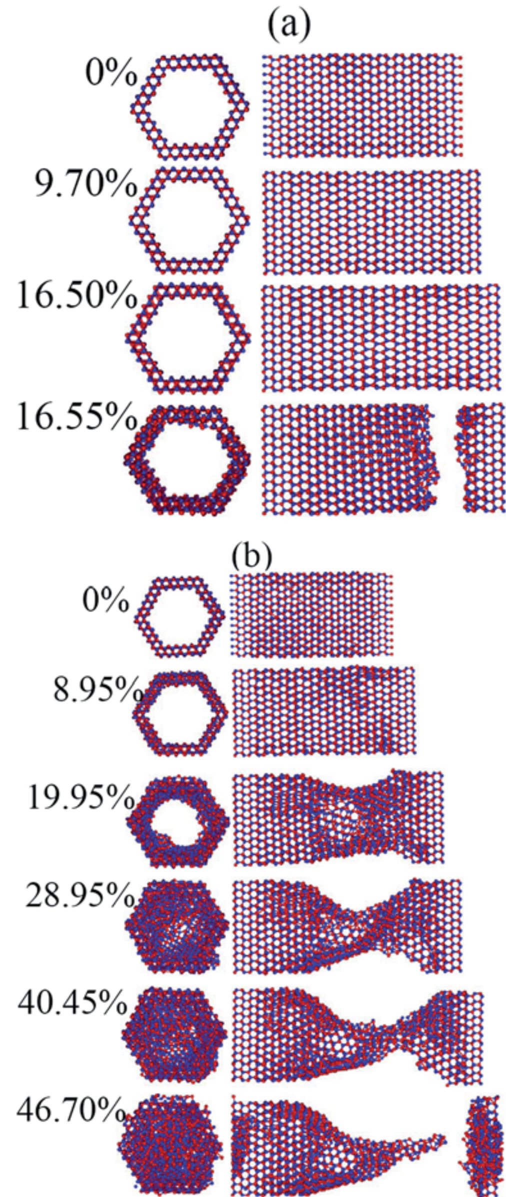

Fig. 4. (Color online) Atomic configuration in selected stages of GaNNTs with thickness of 3.68 Å at temperature of (a) 300 K and (b) 1200 K.

Figures 4a and 4b show the top and side views of the atomic configuration at various stages of the stretching of GaNNTs with thickness of 3.68 Å with strain

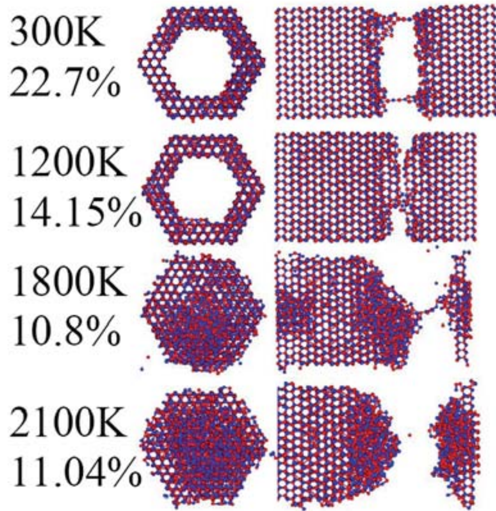

Fig. 5. (Color online) Atomic configuration of GaNNTs with diameter of 6.45 Å as the strain increase to the critical strain at temperature of 300 K, 1200 K, 1800 K and 2100 K.

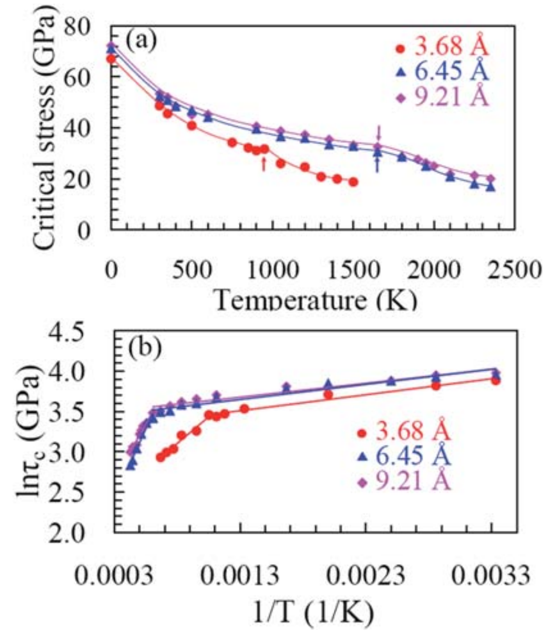

Fig. 6. (Color online) (a) Temperature dependence of the critical stress of GaNNTs. A break appears at a temperature T_c. (b) Evolution of $\ln(\tau_c)$ as a function of the inverse of temperature. The break in each of the plots at a point corresponds to the BDT temperature. BDT temperature increases with increasing the thickness of the GaNNTs.

rate of 0.005%/ps at simulation temperatures 300 K and 1200 K, respectively. Red and blue atoms indicate Ga and N atoms. At 300 K and up to 16.50% elongation, the Ga-N bond lengths increase uniformly and no defects appear in the structures. Upon reaching the critical strain of 16.55%, the crystal structure experiences an abrupt dislocation. And the GaNNTs rupture with a clean cut, no necking is observed. Obviously, at 300 K the tube shows brittle properties. At 1200 K, the extension of the GaNNTs also begins with an elastic deformation from its initial state to the critical strain 8.95%. Necking can be clearly seen with further extension. The necking process develops into several atom thick chains before rupture. The atomic structures near the 'tips' appear much highly disordered. So the GaNNTs show a ductile behavior at 1200 K.

Figure 5 shows the atomic configuration of GaNNTs with diameter of 6.45 Å as the strain increase to the critical strain at temperature of 300 K, 1200 K, 1800 K and 2100 K. The GaNNTs fracture with a clean cut at 300 K and 1200 K and with a necking at 1800 K and 2100 K can be clearly seen. The atomic structures near the 'tips' appear amorphous, which means that plastic deformation takes place through a phase transformation from crystal to amorphous structures. From Figures 4 – 5, we can find that the GaNNTs breaks on a particular side and not in the middle once the strain is applied. It should be noticed that the simulated strain rates in the present work are several orders of magnitude higher than those encountered in experiments. With high strain rate, the interaction among the atoms in the deformed zones has not enough time to transfer to the middle part.

Figure 6a shows the variation in critical stress with the temperature for the GaNNTs. The results clearly show that the critical stress decrease at higher temperatures. Consequently, the mechanical properties of GaNNTs are sensitive to the temperature. As the temperature is increased, a greater number of atoms gain sufficient energy to overcome the activation energy barrier, and hence plastic deformation occurs. This result suggests that a thermally activated process plays an activating role in the complete elongation of GaNNTs. We also can see a break appears at a critical temperatures T_c in the $\tau_c(T)$ curves. Similar experimental results have been found in GaAs [22], InSe [23], SiC [24,25], with breaks in their $\tau_c(T)$ curve at T_c. And T_c closes to the brittle to ductile transition (BDT) temperature of these materials. The results are consistent with the above observations of changes from GaNNTs ruptured with a clean cut at low temperatures to GaNNTs ruptured with necking at higher temperatures under tensile loading.

One way to represent the variations of the yield stress of semiconductor with respect to temperature is to plot $\ln(\tau_c)$ versus $1/T$, as suggested by the kink-diffusion model [26]. In this model, Orowan's equation for the plastic strain rate gives a linear plot with slope that is proportional to the stress-independent activation enthalpy, H, for the glide of the dislocations responsible for crystal deformation. Specifically:

$$\ln\tau_c = \frac{H}{nkT} + \frac{1}{n}[\ln\dot{\varepsilon} - \ln A], \quad (6)$$

where n is related to the stress exponent of the dislocation velocity and A is a constant (see, Ref. [27]). The changes of $\ln(\tau_c)$ as a function of $1/T$ are shown in Figure 6b. There are changes of the slope in the $\ln(\tau_c)$ versus $1/T$ curves at the same temperature, T_c, at which there are breaks in the $\tau_c(T)$ curves. The different slopes

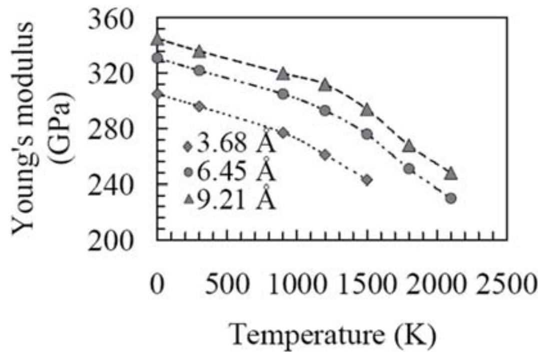

Fig. 7. Young's modulus of the [001]-oriented GaNNTs with {100} side planes at various simulation temperatures.

of the ln $\tau_c\,(1/T)$ curves on the two sides of the transition thus correspond to tow different activation enthalpies, H_t and H_l, for dislocation glide in the high temperature ($T > T_c$) and low-temperature ($T < T_c$) regimes, respectively, which indicates different tensile behavior at low and high temperatures.

Figure 6 also shows that the BDT transition temperature increases with the increasing the thickness of the GaNNTs. The BDT temperatures increase from 900 to 1450 K for the GaNNTs with [100]-oriented lateral facet. The thickness dependence of BDT temperature of GaNNTs maybe associated with large surface to volume ratio of the GaNNTs. The ratio of the numbers of surface atoms to the total number of atoms increases as the thickness of the GaNNTs decreases. The surface atoms have larger energy than the core atoms. So atoms gain sufficient energy to overcome the activation energy barrier, and hence plastic deformation occurs easily in thin GaNNTs.

The Young's modulus can be directly obtained from the ratio of the stress to the strain. The Young's modulus is determined from the results of the tension tests for the strain <2.5 % using linear regression. We get the Young's modulus of the GaNNWs are shown in Figure 7. The Young's modulus of GaNNTs s is distributed within the range 345–230 GPa at the temperature range between 300 K and 2100 K. The values agree well with the experimental result of 227–305 GPa of GaN nanowires [28]. It is shown that the Young's modulus decrease with increasing temperature. The results show that the GaNNTs become softened at higher temperature, since higher temperature corresponds to higher kinetic energy of each atom in average, which will result in easier slipping and elongation of GaNNTs. From Figure 7 we also can see that the Young's modulus decrease with decreasing the thickness of the GaNNTs which is somewhat unexpected. For single-crystal materials, Young's modulus is expected to rather increase with decreasing crystal size [29,30]. The reason to explanation for this behavior is atomic coordination and cohesion near the surface are 'poor' relative to the bulk, and the increasing dominance of the surface would decrease the rigidity of the structure [31].

4 Conclusions

This paper presents the MD simulation of single-crystalline GaNNTs subject to uniaxial tension in the [001] direction. GaNNTs behave different tensile behavior at low temperature and high temperature. The stress-strain curves show that the stresses increase with strain, and decrease abruptly to about 0 GPa at temperature lower than BDT temperature, while decrease gradually with increasing the strain at temperature higher than BDT temperature. The GaNNTs exhibit ductility at high deformation temperatures and brittleness at lower temperature. The BDT temperature depends on the thickness of the GaNNTs, which increased with increasing the thickness of GaNNTs. The BDT temperatures increase from 900 to 1450 K for the GaNNTs. The GaNNTs have lower critical stress and corresponding smaller strain at high temperature than at low temperature, and the critical stress increases with the increasing of the thickness of GaNNTs. Plastic deformation takes place through a phase transformation from crystal to amorphous structures.

Z.G. Wang and X.T. Zu are grateful for the National Natural Science Foundation of China (10704014) and the Program for Innovative Research Team in UESTC. F. Gao and W.J. Weber were supported by the Division of Materials Sciences and Engineering, Office of Basic Energy Sciences, US Department of Energy under Contract DE-AC05-76RL01830.

References

1. A.P. Alivisatos, Science **271**, 933 (1996)
2. J.M. Krans, J.M. van Rutenbeek, V.V. Fisun, I.K. Yanson, L.J. de Jongh, Nature **375**, 767 (1995)
3. Y.N. Xia, P.D. Yang, Y.G. Sun, Y.Y. Wu, B. Mayers, B. Gates, Y.D. Yin, F. Kim, H.Q. Yan, Adv. Mater. **15**, 353 (2003)
4. J.C. Johnson, H.J. Choi, K.P. Knutsen, R.D. Schaller, P.D. Yang, R.J. Saykally, Nature Materials **1**, 106 (2002)
5. H. Morkoc, S. Strite, G.B. Gao, M.E. Lin, B. Sverdlov, M. Burns, J. Appl. Phys. **76**, 1363 (1994)
6. J. Goldberger, R.R. He, Y.F. Zhang, S. Lee, H.Q. Yan, H.J. Choi, P.D. Yang, Nature (London) **422**, 599 (2003)
7. B.D. Liu, Y. Bando, C.C. Tang, G.Z. Shen, D. Golberg, F.F. Xu, Appl. Phys. Lett. **88**, 093120 (2006)
8. J.Q. Hu, Y. Bando, D. Golberg, Q.L. Liu, Angew. Chem. Int. Ed. **42**, 3493 (2003)
9. S.C. Hung, Y.K. Su, S.J. Chen, L.W. Ji, T.H. Fang, L.W. Tu, M. Chen, Appl. Phys. A **80**, 1607 (2005)
10. V.V. Ivanovskaya, N. Ranjan, T. Heine, G. Merino, G. Seifert, Small **1**, 399 (2005)
11. C.Y. Wei, K. Cho, D. Srivastava, Appl. Phys. Lett. **82**, 2512 (2003)
12. C.Y. Wei, K. Cho, D. Srivastava, Phys. Rev. B **67**, 115407 (2003)
13. K.M. Liew, C.H. Wong, M.J. Tan, Acta. Mater. **54**, 225 (2006)
14. Y.R. Jeng, P.C. Tsai, T.H. Fang, Nanotechnology **15**, 1737 (2004)

15. Z.G. Wang, X.T. Zu, F. Gao, W.J. Weber, Appl. Phys. Lett. **89**, 243123 (2006)
16. F. Stillinger, T.A. Weber, Phys. Rev. B **31**, 5262 (1985)
17. J. Kioseoglou, H.M. Polatoglou, L. Lymperakis, G. Nouet, Ph. Komninou, Comput. Mater. Sci. **27**, 43 (2003)
18. B. Xu, A.J. Lu, B.C. Pan, Q.X. Yu, Phys. Rev. B **71**, 125434 (2005)
19. B. Xu, B.C. Pan, J. Appl. Phys. **99**, 104314 (2006)
20. Z.G. Wang, X.T. Zu, F. Gao, W.J. Weber, J. Appl. Phys. **100**, 063503 (2006)
21. J.M. Haile, *Molecular Dynamics Simulation* (Wiley, New York, 1992)
22. T. Suzuki, T. Yasutomi, T. Tokuoka, I. Yonenaga, Phil. Mag. A **79**, 2637 (1999)
23. T. Suzuki, T. Yasutomi, T. Tokuoka, I. Yonenaga, Phys. Stat. Sol. (a) **171**, 47 (1999)
24. P. Pirouz, A.V. Samant, M.H. Hong, A. Moulin, L.P. Kubin, J. Mater. Res. **14**, 2783 (1999)
25. M. Zhang, H.M. Hobgood, J.L. Demenet, P. Pirouz, J. Mater. Res. **18**, 1087 (2003)
26. J.P. Hirth, J. Lothe, *Theory of Dislocations*, 2nd edn. (Wiley, New York, 1982)
27. J. Ravier, A. George, Rev. Phys. Appl. **22**, 1327 (1987)
28. C.Y. Nam, P. Jaroenapibal, D. Tham, D.E. Luzzi, S. Evoy, J.E. Fisher. Nano Lett. 6, 153 (2006)
29. A.J. Kulkarni, M. Zhou, F.J. Ke, Nanotechnology **16**, 2749 (2005)
30. C.Q. Chen, Y. Shi, Y.S. Zhang, J. Zhu, Y.J. Yan, Phys. Rev. Lett. **96**, 075505 (2006)
31. M. Schmid, W. Hofer, P. Varga, P. Stoltze, K.W. Jacobsen, J.K. Nørskov, Phys. Rev. B **51**, 10937 (1995)